FFI-rapport 2013/01807

Seabed characterization with a small towed array – simulation of system design factors

Dag Tollefsen

FFI Forsvarets forskningsinstitutt

Seabed characterization with a small towed array – simulation of system design factors

Dag Tollefsen

Norwegian Defence Research Establishment (FFI)

1 July 2013

FFI-rapport 2013/01807

1129

P: ISBN 978-82-464-2282-4

E: ISBN 978-82-464-2283-1

Keywords

Akustikk

Geoakustikk

Bayes statistikk

Antenne - tauet

Approved by

Torgeir Svolsbru	Project Manager
Elling Tveit	Director

English summary

This report studies design factors for a small activated towed-array system for use in seabed characterization. By seabed characterization is here meant the estimation of geo-acoustic parameters including sound speed, density, and attenuation profiles, and layer thicknesses of the upper few meters of the seabed. The effect of system design factors such as array length (16–48 m), number of hydrophones (3–33), system height above the seabed (10–20 m) and acoustic source frequency content (0.5–4 kHz) are studied by use of simulated data for a modeled activated towed-array system. The signal processing technique applied is matched-field inversion of hydrophone data. A Bayesian inverse method based on Markov-chain Monte Carlo sampling for posterior probability densities is used, which allows for quantified comparisons of effects of individual system factors on the geo-acoustic information content of data.

Based on the simulations in this report for a typical Continental Shelf type seabed, we find that a critical design factor is the distance between the acoustic source and the array, which preferably should be on the order of 30 to 60 m (measured to the closest array element). However, shorter distance does not necessarily preclude meaningful information content. It is shown that the information content decreases with reduced array length and with reduced number of array elements, with a length of 32 m and 33 elements an apparent practical lower limit for meaningful information content of data. The results from and methods applied in this report can be further used in design of small systems for seabed characterization, e.g., an activated towed array system for an autonomous underwater vehicle.

Sammendrag

Denne rapport studerer designfaktorer for et lite aktivert tauet-antenne system for bruk til havbunnskarakterisering. Med havbunnskarakterisering menes her estimering av geofysiske og geoakustiske parametere i de øvre 1-5 metere av havbunnen, herunder lagdeling og profiler for lydhastighet, tetthet og lydbølgedempning. Dette er relevant for å forstå og forutsi havbunnens innvirkning på akustisk transmisjon samt for å prediktere aktive sonaroperasjoner i grunne farvann. Informasjonen kan benyttes i *Rapid Environmental Assessment* målekampanjer.

Rapporten tar utgangspunkt i et modellert system bestående av en aktiv kilde og en kort tauet antenne. Effekten av systemdesignfaktorer som antennelengde (16–48 m), antall hydrofoner (3-33), avstand over havbunnen (10–20 m) og kildefrekvens (0.5–4 kHz) på informasjonsinnholdet i data blir studert. I prosesseringen benyttes miljøtilpasset signalbehandling og en Bayesisk inversjonsmetode basert på Markov-kjede Monte Carlo sampling. Metoden muliggjør kvantifisert sammenligning av effekten av ulike designfaktorer på informasjonsinnholdet i data.

Basert på simuleringene, her for en typisk Kontinentalsokkel type havbunn, finner vi at en viktig designfaktor er avstanden mellom den akustiske kilden og antennen. Denne bør være 30–60 m, målt til nærmeste antenneelement, imidlertid vil ikke kortere avstander nødvendigvis forhindre meningsfullt informasjonsinnhold. Informasjonsinnholdet avtar med redusert antennelengde og med redusert antall antenneelementer, med 32 m lengde og 33 elementer som praktiske nedre grenser for informative data. Effekten av kildens frekvensinnhold blir også studert. Det vises at god oppløsning av relevante havbunnsparametere kan oppnås med et godt designet system. Resultatene og metoden kan videre benyttes i en detaljert studie av, for eksempel, et system for en autonom undervannsfarkost. Inversjonsmetoden kan tilpasses for anvendelse på måledata.

Contents

1 Introduction

Military sonar operations in shallow water are limited by bottom interaction, hence an increasing interest in remote sensing techniques and methods to infer relevant bottom geophysical and geoacoustic properties from acoustic measurements. Much work has hitherto employed large-scale experiment equipment such as deployed or towed acoustic arrays of typical lengths 100-1000 m and deployed or towed acoustic sources. Recent interest has focused on smaller-scale equipment that can be operated in closer proximity to the seabed, e.g. the reflection-coefficient technique by Holland and Osler [1]. A relevant advancing technology for the development of such smaller-scale systems is thin-line arrays [2]; this technology opens the possibility for array systems for lightweight platforms such as an autonomous underwater vehicle (AUV) and ocean gliders. An AUV equipped with a towed array and an acoustic source can be used for seabed characterization, with the recorded acoustic array data inverted for seabed properties/parameters.

A pertinent question for the development of such smaller-scale systems is design in terms of factors such as source frequency content, array length and number of hydrophones and system tow depth, and the geoacoustic information content of data dependence on these factors. This report addresses this topic in the context of simulated data for a modeled towed-array system. The signal processing technique applied is matched-field processing of complex hydrophone data. A Bayesian inverse method is employed that uses Markov-chain Monte Carlo sampling for posterior probability densities interpreted for model parameter estimates and their uncertainties. This makes possible quantified comparisons of the effect of system factors on data information content.

This report is organized as follows.[1] Chapter 2 presents a brief overview of open documented small towed-array technologies (as per fall of 2009). Chapter 3 outlines the Bayesian inverse method. Chapter 4 presents the simulation environment and results for a set of examples. Chapter 5 summarizes the findings of this report.

2 Small towed arrays

A literature survey (per November 20, 2009) revealed several towed array systems for AUVs or other lightweight platforms. A short synopsis of this information is collected in Table 2.1. CMRE (then NURC) at the time had several arrays in development, including the SLITA array [3], and the TriBens with triplets of hydrophones. Some of the arrays were also fitted with other (non-acoustic) types of sensors. Note that not all reports found in this literature survey showed results with actual recorded acoustic data. A review of thin-line array technologies in development was presented by Jespers at a special session at the ECUA in 2010 [2].

[1] This report is based on the presentation "Geoacoustic information content of HLA data" held at the EDA Workshop "Thin Line Arrays Research & Technology (TLAT)", Brussels, 24-25 Nov 2009.

Institution	System Name	Year	Platform	Cable Length [m]	Acoustic Section Length [m]	Element spacing [m]	Acoustic Elements
NURC	SLITA	2007	OEX-AUV	42	37.5	0.211, 0.422	2 x32 48 total
SPAWAR		2005	Slocum Glider	33	23	1	15
ARL-Singapore		2007	REMUS	20	12	0.375,0.75,1.5	11
Woods Hole	RTAS	2006	REMUS	30	9.2	0.75	6 pairs
MIT	DURIP	2006	Bluefin21	76	30	0.75, 1.5	32

Table 2.1 Short towed arrays as of 2009 and some key system parameters. Based on a literature survey (Google per November 2009).

Figure 2.1 shows a sketch of the SLITA array at CMRE as used with the OEX-AUV [4]. The towed array has an active section of 32-m length and is towed approximately 20 m behind the OEX vehicle (measured from the vehicle propeller to the closest acoustic element).

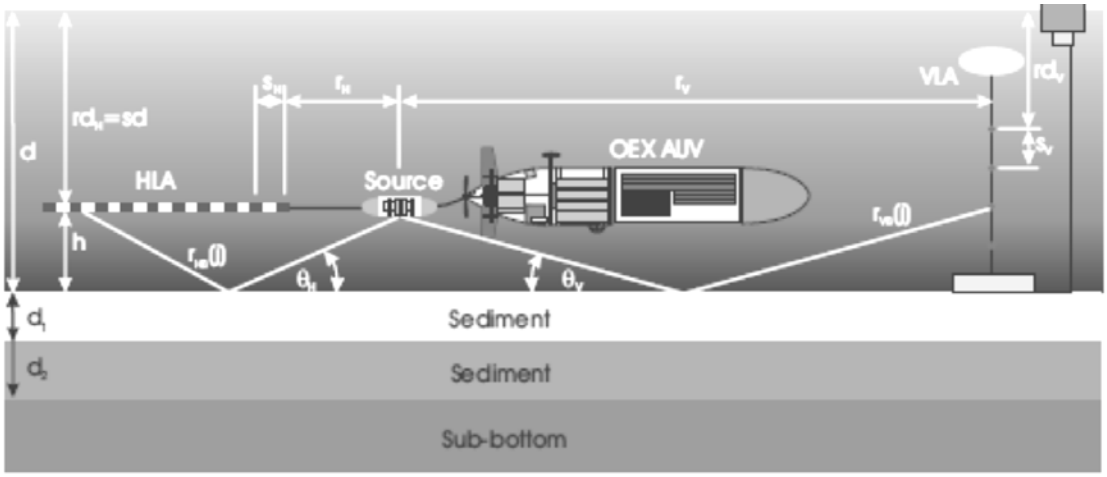

Figure 2.1 Schematic of activated towed array system used at NURC (now CMRE) during a 2009 experiment. (Picture taken from [4]).

For seabed characterization the system in addition uses an active acoustic source. CMRE experimented in 2007 with acoustic sources fitted inside the hull of the AUV [5], with some unfavorable resonance effects occurring. For a subsequent experiment, the towed source body TOSSA had been developed, with experiment results reported in [6] and [7].

3 Bayesian Inversion

This section briefly summarizes Bayesian matched-field geoacoustic inversion as applied in this report. A complete treatment can be found in [8], see also [9] for an application to large horizontal line arrays.

Let vectors representing the model (here, set of geoacoustic parameters) and data (here, complex acoustic fields at a sensor array) be denoted **m** and **d,** respectively. Bayes rule may be expressed

$$P(\mathbf{m} \mid \mathbf{d}) \propto P(\mathbf{d} \mid \mathbf{m}) P(\mathbf{m}), \tag{3.1}$$

where $P(\mathbf{m}|\mathbf{d})$ is the posterior probability density (PPD) and $P(\mathbf{m})$ is the prior distribution, and a fixed normalization factor has been omitted. For measured data, $P(\mathbf{d}|\mathbf{m})$ is interpreted as a function of **m**, the likelihood function, which can generally be expressed $L(\mathbf{m}) \propto \exp[-E(\mathbf{m})]$ where E is the data misfit function. The data and prior can be combined to form a generalized misfit, $\phi(\mathbf{m},\mathbf{d}) = E(\mathbf{m},\mathbf{d}) - \log P(\mathbf{m})$, and the PPD written

$$P(\mathbf{m} \mid \mathbf{d}) = \frac{\exp[-\phi(\mathbf{m},\mathbf{d})]}{\int \exp[-\phi(\mathbf{m}',\mathbf{d})] d\mathbf{m}'}, \tag{3.2}$$

where the domain of integration spans the parameter space. The multi-dimensional PPD is typically interpreted in terms its integral quantities. Of interest here are marginal probability distributions, defined

$$P(m_i \mid \mathbf{d}) = \int \delta(m_i - m_i') P(\mathbf{m}' \mid \mathbf{d}) d\mathbf{m}', \tag{3.3}$$

where δ is the Dirac delta function. Also of interest is the width Δ of the 95% highest probability density (HPD) credibility intervals; the interval of minimum width containing 95% of the marginal probability. For nonlinear problems an analytic solution to the integral in Eq. 3.3 is generally not available and numerical methods must be applied. The integral is solved here using the Markov-chain Monte Carlo method of Metropolis-Hastings sampling in rotated coordinates.

The likelihood function is defined by specifying the data error distribution. For multi-frequency acoustic data, $\mathbf{d} = \{\mathbf{d}_f, f=1, F\}$, the standard assumptions of uncorrelated complex-Gaussian distributed errors with variance ν_f at the f th frequency and unknown source amplitude and phase lead to data misfit function[2]

$$E(\mathbf{m}) = \sum_{f=1}^{F} B_f(\mathbf{m}) / \nu_f, \tag{3.4}$$

[2] This misfit function uses maximum-likelihood estimates for source amplitude and phase, i.e., prior knowledge of the source strength and spectrum is not required. Other maximum-likelihood based misfit functions can be derived and applied.

where $B_f(\mathbf{m})$ is the Bartlett mismatch defined by

$$B_f(\mathbf{m}) = \mathrm{Tr}\{\mathbf{C}_f\} - \frac{\mathbf{d}_f^\dagger(\mathbf{m})\mathbf{C}_f\mathbf{d}_f(\mathbf{m})}{|\mathbf{d}_f(\mathbf{m})|^2}. \tag{3.5}$$

Here, Tr{•} represents the matrix trace, † represents conjugate transpose, $\mathbf{d}_f(\mathbf{m})$ is the replica acoustic field computed for model **m,** and $\mathbf{C}_f$ is the data cross-spectral density matrix (CSDM) at the *f*th frequency. To simulate noisy data, the CSDM can be computed using synthetic acoustic fields for the true model and the error variance added to the main diagonal of $\mathbf{C}_f$, i.e.,

$$\mathbf{C}_f = \mathbf{d}_f\mathbf{d}_f^\dagger + \nu_f\mathbf{I}, \tag{3.6}$$

where **I** is the identity matrix. Under the assumption of independent Gaussian errors, data variances that are representative of experimental data can be computed as

$$\nu_f = |\mathbf{d}_f|^2\, 10^{-\mathrm{ESNR}_f/10} / N \tag{3.7}$$

where *N* the number of array elements and ESNR is the equivalent signal-to-noise ratio which takes into account all sources of uncertainty, including measurement and theory error. ESNR values can be computed according to

$$\mathrm{ESNR}_f = 10\log_{10}\frac{\mathrm{Tr}\{\mathbf{C}_f\} - B_f(\hat{\mathbf{m}})}{B_f(\hat{\mathbf{m}})}, \tag{3.8}$$

where $B_f(\hat{\mathbf{m}})$ is the Bartlett mismatch for an optimal geoacoustic model estimate $\hat{\mathbf{m}}$. Optimal mismatch values reported in the literature (with array lengths 100−1000 m) translate to ESNR values of 0–8 dB, and typically decrease with increasing frequency. For small array systems as studied in this report there are (as of 2009) no results available. A conservative estimate for ESNR of 4 dB (reduced to 2.5 dB at the highest frequency) is used in this report.

4 Examples

4.1 Model environment

An environmental model representative of the shallow continental shelf was chosen for this study. The environment (Figure 4.1) consists of a 115-m water column over a seabed with a 3-m thick sediment layer over a semi-infinite basement. A downward refracting sound-speed profile in water is assumed, with sound speed decreasing from 1472 m/s at the surface to 1468 m/s at the seabed. Sound speed in the sediment increases from 1503 m/s at the seabed to 1528 m/s at 3 m depth (an increase with depth z given by $z^{0.015}$, typical of sandy sediments). The sound speed in the basement is 1750 m/s, representative of consolidated sediment.

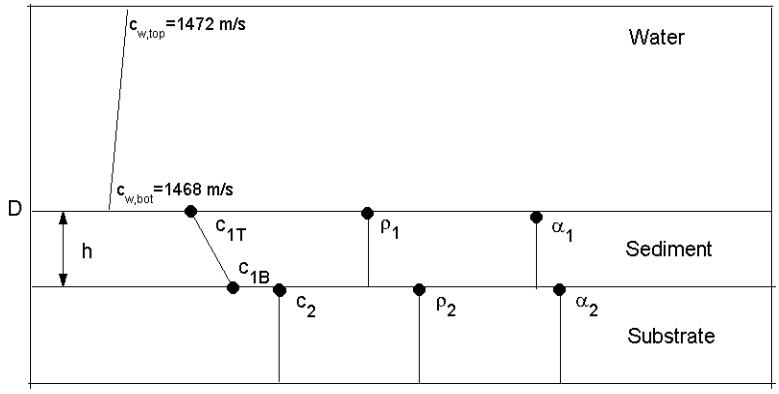

Figure 4.1 Model of the Continental shelf used for this study. See text for explanation.

The true values and a priori uniform search bounds for the eight seabed parameters are given in Table 4.1. Source-array range, source depth, array depth, water depth, and sound speed in the water column are fixed to their true values. The normal-mode numerical propagation model ORCA [9] was used to compute synthetic data and replica pressure fields in all cases.

Parameter Name	Symbol	Unit	Lower Bound	Upper Bound	True Value
Sediment thickness	h	m	0	12	3
Sediment p-velocity surface	c_{1T}	m/s	1450	1600	1503
Sediment p-velocity bottom	c_{1B}	m/s	1450	1650	1528
Substrate p-velocity	c_2	m/s	1600	1900	1750
Sediment density	ρ_1	g/cm³	1.20	2.00	1.50
Substrate density	ρ_2	g/cm³	1.40	2.20	1.85
Sediment p-wave attenuation	α_1	dB/λ	0.01	1.00	0.22
Substrate p-wave attenuation	α_2	dB/λ	0.01	1.00	0.12

Table 4.1 Geoacoustic model parameters, prior search bound, and true values for the simulation study.

A number of source and array configurations are considered in a set of examples in the following. These cases are compared to a baseline case which involves a 32-m length HLA with 33 sensors

spaced at 1-m intervals, with the acoustic source and the array at 105-m depth (10 m above the seafloor) and 30-m range from the closest array element.
The baseline case considers an omnidirectional source in the frequency band 0.8–1.4 kHz, with an alternative frequency band of 2.5–3.1 kHz. (To limit computational efforts, a frequency spacing of 0.1 kHz is used in the processing.)

4.2 System parameters

We are interested in an activated towed-array system for seabed characterization. There are several systems factors that can be varied. In the following these factors are examined:

- Source frequency band
- Array length
- Number of hydrophones
- System height above seafloor
- Source-array separation.

The source-array separation (henceforth also denoted *scope*) is here measured from the acoustic source to the closest array element. For this simulation study we model an omnidirectional source with the specified frequency content. Table 4.2 provides system parameters that were varied in the simulations.

Parameter	Symbol	Unit	Baseline	Alternative
Array length	L	m	32	16, 48
Number of sensors	N		33	17, 9, 3
Scope	r_H	m	30	10, 60
Height above seabed	rd	m	10	20
Source frequencies		kHz	0.8–1.4	0.5–0.8, 2.5–3.1

Table 4.2 System parameters varied in the simulations.

The system height above seabed and source-array distance determines the grazing angles sampled by the acoustic array. The grazing angles are given by:

$$\theta = \tan^{-1}\left(\frac{2 * rd}{r_H + (n-1) * s_H} \right), \tag{4.1}$$

where rd is the system (array and source) height above the seabed, r_H is the source-array distance, s_H is the hydrophone separation and n is the element number $1 \le n \le N$. In geoacoustic inversion studies, it is often assumed that an informative system should sample at least up to the critical angle for transmission into the seabed; the critical angle is 10−35° for the types of sediment typically encountered on the Continental Shelf.

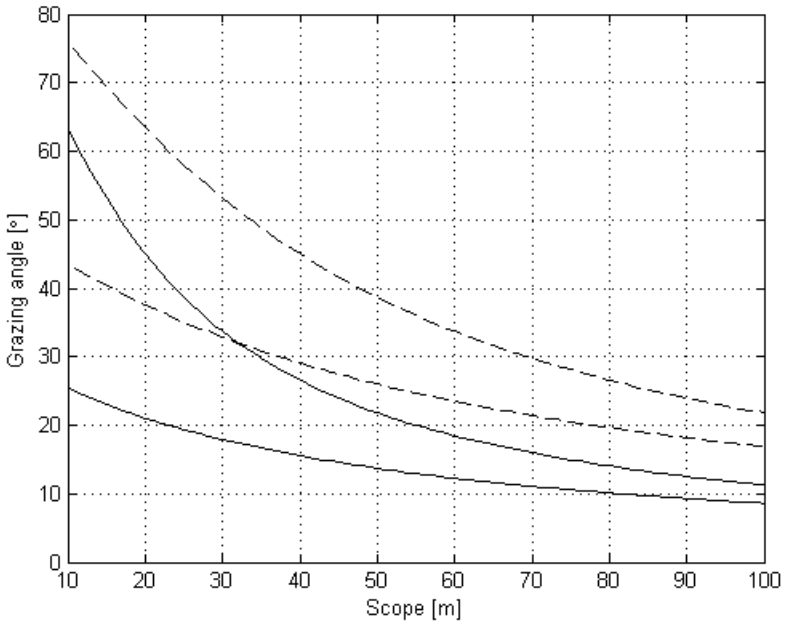

Figure 4.2 Interval of sampled grazing angles (interval between by two lines) as a function of source-receiver separation (scope) for a 32-m length array at tow height 10 m (solid lines) and 20 m (broken lines) above the seabed.

Figure 4.2 shows the interval of sampled grazing angles as a function of scope for the baseline system parameters (Table 4.2) for system heights 10 m and 20 m above the seabed. The figure indicates that in order to sample low grazing angles one should select *low height above the seafloor* and *long scope*. For the environment of Table 4.1, the critical angle is ~12°; Fig. 4.2 shows that to achieve sampling around the critical angle would require a scope in excess of approximately 50 m for the baseline system. However, this discussion does not take into account information carried by steep-angle (above-critical) energy. Furthermore, there is no apparent simple relation between sampling of grazing angles and geoacoustic information content; this further motivates the inversion study carried out in the following.

4.3 Results

Figures in the following show one-dimensional marginal PPDs for the eight unknown seabed model parameters, for three simulations in each figure. In each of the simulations, one system parameter has been varied, with the remaining held at their baseline (fixed) values. The figures provide a means to compare the geoacoustic information content dependence on system factors.

4.3.1 Source-array separation

First, we examine the effect of source-array separation. Previous studies for a fixed array configuration indicated that the source-receiver distance can have a profound effect on geoacoustic information content [9].

Figure 4.3 shows marginal PPDs for eight geoacoustic parameters for scope of: (a) 10 m, (b) 30 m, and (c) 60 m, for the mid-frequency source (0.8−1.4 kHz). For 10-m scope, the sediment thickness (h) is well resolved but there is relatively little information on other seabed parameters as indicated by their wide distributions over the entire *a priori* intervals. For 30-m scope, there is increased information on the sound speed profile in the seabed (defined by the parameters h, c_{1T}, c_{1B}, and c_2), and some information on sediment density (ρ_1) and attenuation (α_1). For 60-m scope, the sound speed profile in the seabed is well resolved with sediment attenuation also resolved.

Figure 4.4 shows marginal PPDs for eight geoacoustic parameters for scope of: (a) 10 m, (b) 30 m, and (c) 60 m, for the high-frequency source (2.5−3.1 kHz). Overall, the information content is slightly higher (as indicated by narrower marginal distributions) than the corresponding cases for the mid-frequency source (Fig. 4.3). In particular, note that with 10-m scope (Fig. 4.4 (a)), the sediment sound speed structure (defined by the parameters h, c_{1T}, and c_{1B}), and sediment density and attenuation (ρ_1 and α_1) is better resolved that for the mid-frequency source (Fig. 4.3 (a)). Although both sources sample the same spectrum of grazing angles (approximately 25° to 62°), the high-frequency source presumably provides more information from steeper-angle, higher-order bottom-interacting modes than the mid-frequency source.

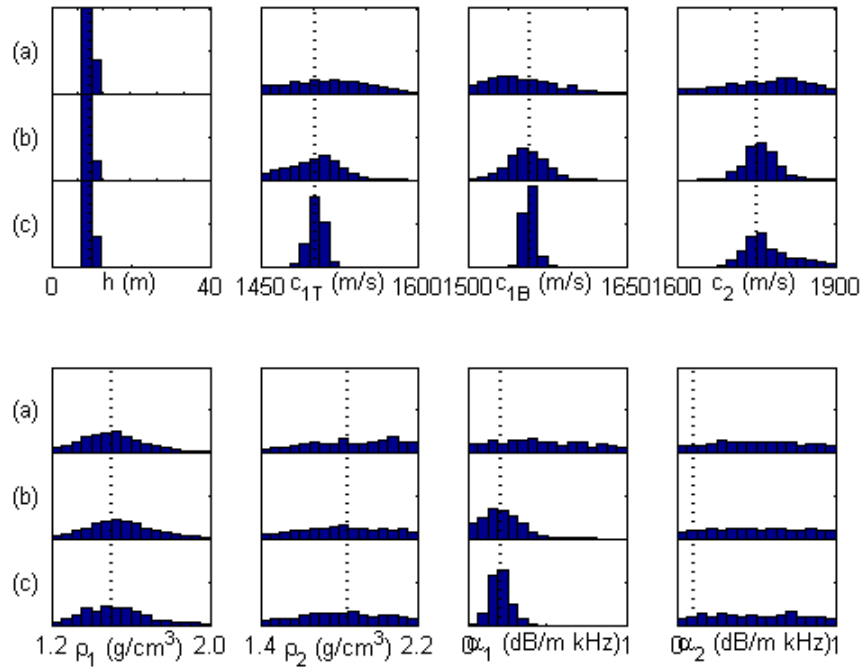

Figure 4.3 *Effect of source-array separation. Marginal PPDs for canonical case with mid-frequency source (0.8−1.4 kHz) and 32-m array for source-array separation of: (a) 10 m, (b) 30 m, (c) 60 m. Dotted lines indicate true parameter values.*

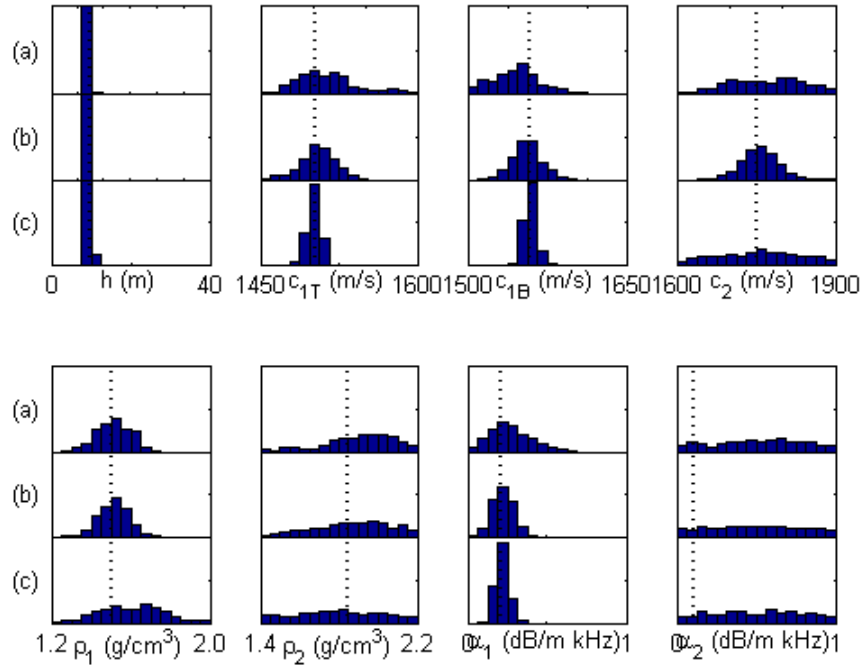

Figure 4.4 *Effect of source-array separation, high-frequency source (2.5−3.1 kHz). Marginal PPDs for 32-m array for source-array separation of: (a) 10 m, (b) 30 m, (c) 60 m. Dotted lines indicate true parameter values.*

4.3.2 Source frequency content

Next we examine the effect of the frequency content of the source signal, for the most informative source-array separation (60 m) from the previous example. Figure 4.5 presents results, in terms of credibility intervals (95-% HPD widths), for the eight model geoacoustic parameters for source frequency bands of (a) 0.5−0.8 kHz, (b) 0.8−1.4 kHz, and (c) 2.5−3.1 kHz. To limit computation time, in all cases seven frequency components of the signal were modeled, with frequency spacing 50 Hz for the low-frequency source and 100 Hz for the mid- and high-frequency sources.

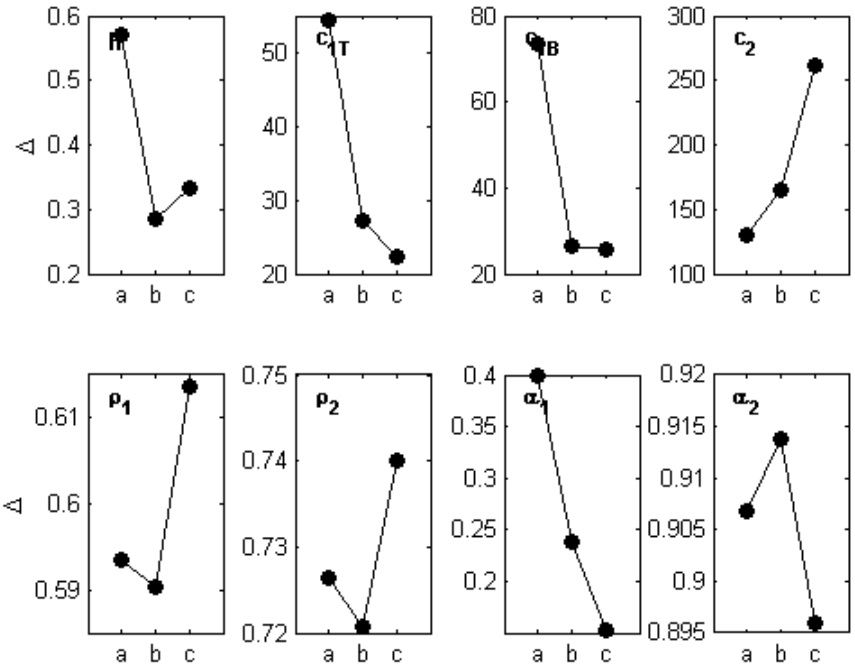

Figure 4.5 Effect of source frequency content. 95% HPD credibility intervals for 32-m array and scope 60 m and data consisting of: (a) 0.5−0.8 kHz band with 50-Hz spacing, (b) 0.8−1.4 kHz band with 100-Hz spacing, and (c) 2.5−3.1 kHz with 100-Hz spacing

From Fig. 4.5 one can observe that the low-frequency source, case (a), provides less informative results when compared with the mid-frequency and high-frequency sources, cases (b) and (c). For example, the credibility intervals increase from 0.3 to 0.6 m for h, 27 to 54 m/s for c_{1T}, and 26 to 73 m/s for c_{1B} (values for low- and mid-frequency sources, respectively). In contrast, for substrate sound speed (c_2) the credibility interval decreases from 164 to 130 m/s; this agrees with the assumption that lower-frequency signals penetrate deeper into the seabed and carry more information on deeper structure of the seabed. For the high-frequency source, case (c), the changes in credibility intervals are for most parameters small when compared to the mid-frequency source, case (b), however, for substrate sound speed (c_2) the credibility interval increases from 164 m/s (mid-frequency source) to 262 m/s (high-frequency source).

4.3.3 Array length and number of elements

Array length, number of elements, and inter-element separation are important design factors. To limit the number of cases studied, equidistant spacing is assumed, i.e., $d=L/(N-1)$, with d the element spacing, L the array length, and N the number of elements. Furthermore, three array lengths (16, 32, and 48 m) are studied with the number of elements fixed to 33 (element spacing varying with array length), and the effect of number of array elements is studied for a 32-m length array only.

The effect of array length was studied for 33-sensor arrays. The simulations were done for the baseline system parameters of Table 4.2, with 16, 32, and 48 m length; note that element spacing varied for these cases. Figure 4.6 shows 95-% HPD widths for eight geoacoustic parameters for (a) 16, (b) 32, and (c) 48 m array length. The figure shows that the information content in general increases with increased array length, with highest information content for the 48-m array. Resolution of the sound speed profile in the seabed (defined by the parameters h, c_{1T}, c_{1B}, and c_2) increases with increasing array length; note also a significant increase in resolution of sediment attenuation (α_1) with array length.

The effect of number of sensors was studied for a 32-m length array. The simulations were done for the baseline system parameters of Table 4.2, with 3, 9, 17, and 33 hydrophones respectively, such that equidistant (but varying between the cases) spacing was maintained. Figure 4.7 shows 95-% HPD widths for eight geoacoustic parameters for (a) 3, (b) 9, (d) 17, and (d) 33 elements. The figure shows that the information content decreases with reduced number of elements, with substantial improvement in information content when increasing from 17 elements (2-m spacing) to 33 elements (1-m spacing).

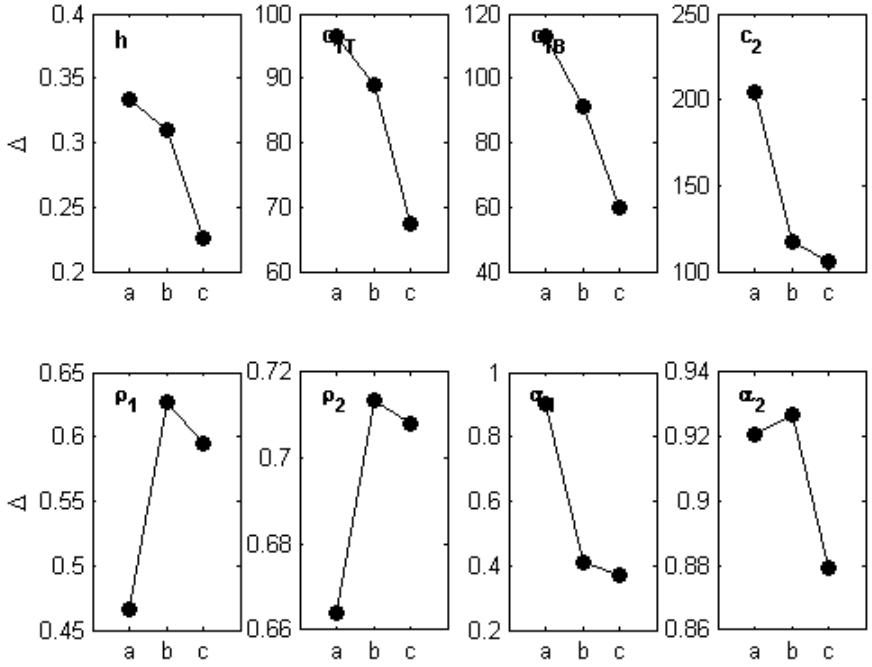

Figure 4.6 Effect of array length. 95-% HPD widths for 33-sensor array of length: (a) 16 m (0.5-m spacing), (b) 32 m (1-m spacing), (c) 48 m (1.5-m spacing).

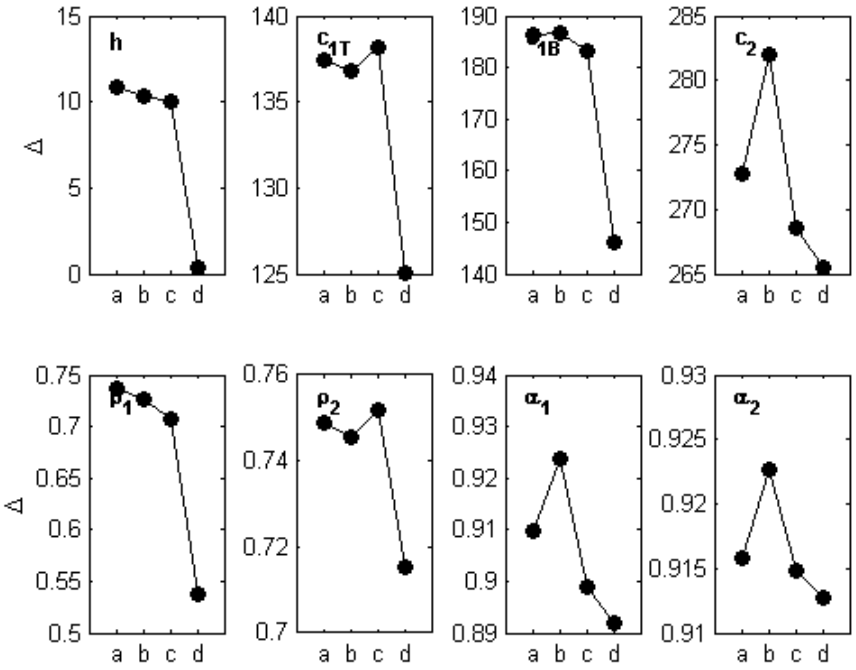

Figure 4.7 Effect of number of sensors. 95-% HPD widths for: (a) 3 sensors at 16-m spacing, (b) 9 sensors at 4-m spacing (c) 17 sensors at 2-m spacing, (d) 33 sensors at 1-m spacing.

4.3.4 Uncertainty estimates

Geoacoustic parameter estimates can be quantified in terms of mean with mean-deviation uncertainties. Table 4.3 shows estimates for the mid-frequency and high-frequency sources with the baseline array (scope 30 m, array length 32 m, 33 sensors) for six of the geoacoustic model parameters.

Parameter and unit	True value	Mid-frequency source 0.8−1.4 kHz	High-frequency source 2.5−3.1 kHz
h (m)	3	3.0±0.1	3.0±0.1
c_{1T} (m/s)	1503	1503±6	1501±5
c_{1B} (m/s)	1528	1528±6	1529±6
c_2 (m/s)	1750	1772±35	1755±62
ρ_1 (g/cm^3)	1.50	1.52±0.12	1.60±0.13
α_1 (dB/λ)	0.22	0.21±0.05	0.22±0.03

Table 4.3 Geoacoustic parameter estimates in terms of mean estimates with mean-deviation uncertainties from Bayesian inversion of simulated data for a 32-m length, 33-sensor towed-array system for two source frequency bands.

4.4 Other factors

Further simulations (not shown) indicated that for the canonical array, higher ESNR (6 dB) did not have a significant effect on information content, whereas lower ESNR (0 dB) give wider distributions for all parameters and in general poor information content. Data error correlations, i.e., spatial correlations of data errors between sensors, are not explicitly accounted for in the inversion method used in this report. This can in general lead to an under-estimation of model parameter uncertainties (if error correlations are present). Techniques to estimate and account for data error correlations in Bayesian inversion have been developed and applied elsewhere. In all simulations in this report, system geometric parameters and water depth were for simplicity fixed to their nominal values. Thus the effect of uncertainties in geometric parameters on geoacoustic information content has not been explicitly accounted for (a combined effect is included via the equivalent signal-to-noise ratio). It may in general be assumed that such effects increase with increasing source frequency, e.g., loss of information content due to array shape deformation, array movement, array tilt, etc., is comparatively larger for a high-frequency source than for a mid/low-frequency source. A separate study should address the potential degrading effect of geometric parameter uncertainty on geoacoustic information content of data to decide whether pre-processing steps to reduce such uncertainties are required.

5 Summary

This report presented results from simulations of a small activated towed-array system for seabed geoacoustic characterization. The processing method employed is Bayesian matched-field inversion of complex pressure data, with no prior assumptions on source amplitude/phase. Key findings are:

- Source-array separation has an important effect on information content of all seabed geoacoustic parameters. Highest information content is obtained with 60-m separation, attributed to increased sampling near the critical angle. With shorter separation, higher information content is obtained with 30-m scope than with 10-m scope.
- Array length and the number of array elements have an important effect on information content, in general such that information content for all seabed parameters is degraded with reduced number of array elements and with reduced array length. For the cases studies here, 32-m array length and 33 elements provide practical lower limits for meaningful results in terms of geoacoustic information content.
- The mid-frequency (0.8−1.4 kHz) and high-frequency (2.5−3.1 kHz) sources resolved well the parameters defining the sound speed structure of sediment (h, c_{1T}, c_{1B}) and substrate (c_2), with somewhat higher information content for the high-frequency source. A low-frequency (0.5−0.8 kHz) source yielded reduced information of all parameters but higher information on the substrate sound speed.

Based on the simulations, we find that a critical design factor is the separation between the acoustic source and the array which preferably should be on the order of 30 to 60 m for the environment and system studied here; however, shorter separation does not necessarily preclude meaningful geoacoustic information content. A practical lower limit on array length is 32 m and a limit on the number of sensors is 33. Optimal combinations of array length, number of elements and inter-element spacing could warrant further studies once upper/lower practical limits have been set from other system design criteria.

The observations made in this report are based on a relatively small set of simulations and for one seabed environment; several other combinations of system parameters and types of seabed environments are possible. Note that alternative data processing methods, e.g., involving pre-filtering of data and the use of prior information on source amplitude/phase can be applied (if available); the intention here has been to simulate a well-established inversion method that is relatively straightforward to apply to experimental data. The Bayesian inversion method employed provides a means to rigorously quantify the effects of system parameters on geoacoustic information content. The method can be adapted and applied to measured data.

Bibliography

[1] C. W. Holland and J. Osler, "High-resolution geoacoustic inversion in shallow water: a joint time- and frequency-domain technique," *J. Acoust. Soc. Am.*, vol. 107, pp. 1263-1279, 2000.

[2] S. Jespers, "An overview of current thin line array technologies and relevant research aspects," *10th European Conference on Underwater Acoustics*, 2010.

[3] A. Maguer, R. Dymond, M. M. Biagini, S. Fioravanti, and P. Guerrini, "SLITA: A new SLim Towed Array for AUV applications," *9th European Conference on Underwater Acoustics*, 2008.

[4] A. Barbagelata, "Thirty years of towed arrays at NURC," *Oceanography*, vol. 21, no. 2, pp. 24-33, 2008.

[5] P. L. Nielsen, C. Harrison, and C. Holland, "Local bottom characterization using an AUV,"NURC-FR-2008-028, 2008.

[6] P. L. Nielsen, Y.-M. Jiang, and C. W. Holland, "An autonomous underwater vehicle for seabed characterization," *MREA10 Conference (geos2. nurc. nato. int/mrea10conf),* 2010.

[7] P. L. Nielsen, C. Holland, and L. Troiano, "Geoacoustic characterization and bottom scattering measurements using an AUV,"CMRE-FR-2012-005, 2012.

[8] S. E. Dosso and J. Dettmer, "Bayesian matched-field geoacoustic inversion," *Inverse Problems*, vol. 27, p. 055009, 2011.

[9] D. Tollefsen and S. E. Dosso, "Geoacoustic information content of horizontal line array data," *IEEE J. Oceanic. Eng.*, vol. 32, pp. 651-662, 2007.